Reactive and Functional Polymers 203 (2024) 106010

Contents lists available at ScienceDirect

Reactive and Functional Polymers

journal homepage: www.elsevier.com/locate/react

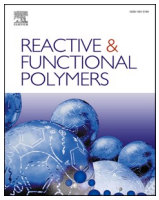

Poly(alkylene 2,4-furanoate)s: The potential of structural isomerism for outstanding sustainable food packaging and unexpected evidence of self-healing microstructure

Enrico Bianchi [a], Michelina Soccio [a,b,c,*], Valentina Siracusa [d], Massimo Gazzano [e], Shanmugam Thiyagarajan [f], Nadia Lotti [a,b,g]

[a] Department of Civil, Chemical, Environmental and Materials Engineering, University of Bologna, Via Terracini 28, 40131 Bologna, Italy
[b] Interdepartmental Center for Industrial Research on Advanced Applications in Mechanical Engineering and Materials Technology, CIRI-MAM, University of Bologna, Viale del Risorgimento 2, 40136 Bologna, Italy
[c] Interdepartmental Center for Industrial Research on Buildings and Construction, CIRI-EC, University of Bologna, Via del Lazzaretto 15/5, 40131 Bologna, Italy
[d] Department of Chemical Science, University of Catania, Viale A. Doria 6, 95125 Catania, Italy
[e] Institute for Organic Synthesis and Photoreactivity, ISOF-CNR, Via Gobetti 101, 40129 Bologna, Italy
[f] Wageningen Food & Biobased Research, Wageningen University and Research, P.O. Box 17, 6700 AA Wageningen, the Netherlands
[g] Interdepartmental Center for Industrial Agro-Food Research, CIRI-AGRO, University of Bologna, Via Quinto Bucci 336, 47521, Cesena, Italy

ARTICLE INFO

Keywords:
2,4-furandicarboxylic acid
2,4-FDCA
2,5-furandicarboxylic acid
2,5-FDCA
Structural isomerism
Thermal properties
Diffractometric analysis
Mechanical properties
Gas barrier properties

ABSTRACT

2,5-furandicarboxylic acid is an extremely appealing renewable chemical building block because of its potential to replace the petrochemical and industrially widespread terephthalic acid via the synthesis of poly(alkylene 2,5-furanoate)s (2,5-PAF). The recent interest in its structural isomer, 2,4-furandicarboxylic acid (2,4-FDCA), opened the study of poly(alkylene 2,4-furanoate)s (2,4-PAF). In this work, 2,4-FDCA was polymerized with linear glycols of increasing chain length, via a solvent-free polycondensation reaction, obtaining high molecular weight 2,4-PAF. Namely, poly(trimethylene 2,4-furanoate) (2,4-PTF), poly(pentamethylene 2,4-furanoate) (2,4-PPeF) and poly(hexamethylene 2,4-furanoate) (2,4-PHF). These polyesters were compression molded into films and subjected to NMR, GPC, WAXS, PLOM, TGA and DSC analyses. The functional properties for food packaging applications were evaluated by mechanical and gas permeability tests. 2,4-PAF had tunable mechanical properties, depending on the glycol used, and in some cases, the mechanical behavior of a thermoplastic elastomer and shape recovery after break. In particular, 2,4-PPeF had outstanding gas barrier properties, while DSC analyses on 2,4-PHF showed an endothermic phenomenon attributed to the isotropization of a partially-ordered phase: it was possible to demonstrate that this phase was disrupted during tensile tests and slowly recovered over time, at room temperature. Overall, the results offer new insights into the structure-property relationships of poly(alkylene 2,4-furanoate)s and display their great potential for the production of biobased, monomaterial, easily recyclable and sustainable food packaging.

1. Introduction

Plastics are an irreplaceable class of materials in many applications because of their unique combination of low specific weight with tunable mechanical behavior, often accompanied by special properties of high added value. 391 Mtons of plastics were produced in 2021 worldwide and packaging had a predominant role in the market, comprising 44% of the total production volume [1]. However, packaging is often single use and fulfills its purpose in a relatively short time window, by protecting other products in their transportation and storage. A short life cycle, fast rate of production and high durability are the causes which concurred to the incontrollable growth of plastic pollution as a major issue for marine ecosystems and, potentially, human health [2,3]. The issue is apparent in the case of food packaging, which is meant to protect goods with a short shelf life, whose recycling is made particularly challenging by the possible contamination of food products and by the multilayered nature of many food packaging systems, which must be structured in an internal layer with high gas barrier properties, typically poly(ethylene

* corresponding author at: Department of Civil, Chemical, Environmental and Materials Engineering, University of Bologna, Via Terracini 28, 40131 Bologna, Italy.
E-mail address: m.soccio@unibo.it (M. Soccio).

https://doi.org/10.1016/j.reactfunctpolym.2024.106010
Received 22 May 2024; Received in revised form 8 July 2024; Accepted 10 July 2024
Available online 14 July 2024

vinyl alcohol) (EVOH), to control the atmosphere to which the food is exposed, with additional outer layers of polymers intended to compensate the insufficient mechanical properties and moisture resistance of EVOH [4,5]. Among the possible solutions, the problem can be tackled with legislative or non-legislative interventions [6,7], and by strengthening the recycling infrastructure. On this front, progress has been made in Europe in recent years, with a 117% growth in the recycling of post-consumer plastic waste between 2006 and 2020 [1], but this progress has not been sufficient to completely stop the flow of plastics landfilled and dispersed in the environment. For this reason, the ecodesign of polymeric materials plays a major role in the smart management of their life cycle, and one way in which Polymer Chemistry can reduce the environmental impact of food packaging is by enhancing its recyclability and circularity, creating a new generation of polymers with combined high mechanical and gas barrier properties, thus suitable for the production of single-component packaging. When designing new green and circular materials, the sustainability of raw materials and carbon emissions must also be taken into consideration: LCA studies have found that the production of 1 metric ton of biobased materials saves 55 GJ of energy and 3 tons of equivalent CO_2, compared to conventional materials [8]. For biobased materials from first-generation biomass (edible crops), lower carbon emissions are counterbalanced by the environmental impact of phosphate and nitrous oxide pollution caused by the use of fertilizers and pesticides [8]. In the future, however, the potential of refineries based on second-generation biomass (non-food crops and lignocellulosic waste) [9] will mitigate this impact, while at the same time representing a great opportunity for circularity. Overall, the current objective of research in the field of food packaging is the prevention of environmental issues related to the production and use of plastic with the smart ecodesign of biobased, single-component and easily recyclable polymers. 2,5-furandicarboxylic acid (2,5-FDCA) has emerged in recent years among the most relevant biobased chemical platforms to achieve this goal: it was in fact selected by the US Department of Energy as the second most promising [10,11] and its production is currently approaching commercial scale [12,13]. In Academia, 2,5-FDCA has been extensively studied, and in particular the polyester resulting from the polycondensation with ethylene glycol, poly(ethylene 2,5-furanoate) (2,5-PEF) [14–19]. The functional properties of PEF were found to be particularly interesting in the field of food packaging, attracting industry attention for its potential as a substitute for petrochemical poly (ethylene terephthalate) (PET). Specifically, one of the most interesting characteristics of 2,5-PEF is its gas barrier properties, 19 times superior to those of PET [20], correlated with the higher rigidity of the furan subunit compared to the terephthalic one, which causes less ring flipping and lower gas permeation [21]. Expanding the scope to the entire class of poly(alkylene 2,5-furanoate)s (2,5-PAF) homopolymers, high molecular weight polyesters were synthesized from 2,5-FDCA and linear glycols of increasing chain length, compression molded into films and characterized by Guidotti et al., with the production of poly(propylene 2,5-furanoate) (2,5-PPF) from 1,3-propanediol, poly(butylene 2,5-furanoate) (2,5-PBF) from 1,4-butanediol, poly(pentamethylene 2,5-furanoate) (2,5-PPeF) from 1,5-pentanediol and poly(hexamethylene 2,5-furanoate) (2,5-PHF) from 1,6-hexanediol [22]. The results were found to be particularly interesting in the case of 2,5-PPeF, which presented an elastomeric behavior with shape recovery and, above all, gas barrier properties comparable to those of EVOH. It has been experimentally demonstrated that a partially ordered mesomorphic phase is responsible for these exceptional results [23], which is theorized to explain the peculiar gas barrier properties of all amorphous and rubbery 2,5-PAFs. In some instances, bifuran polymers were also theorized to derive excellent gas barrier properties from other kinds of interactions originated by oxygen exposure [24] and difuran polymers showed comparably good gas barrier properties [25]. In this context, a Henkel-type thermal disproportionation was studied by S. Thiyagarajan et al. as a new synthetic method to obtain 2,5-FDCA from second-generation biomass [23]. As a serendipitous discovery, 2,4-FDCA, a structural isomer of 2,5-FDCA could be obtained as a co-product of the reaction, with a selectivity ranging from 14 to 30%, depending on the catalyst used. In silico and dielectric spectroscopy experiments were also carried out on both 2,5-PAF [26–31] and 2,4-PAF [32–34]. Moreover, the synthesis of 2,4-PAF and several copolyesters was carried out, but their molecular weight was not suitable for the functional characterization of food packaging applications [35–37]. Another side product of the reaction studied by S. Thiyagarajan et al. [23] was furan, a high-added value chemical that can be further valorized by transformation into 1,4-butanediol [38]. For this reason, as proof of concept for a green process with high atom economy, Bianchi et al. decided to study the potential of the homopolymer obtained from the dimethyl ester of 2,4-FDCA and 1,4-butanediol for food packaging applications: compared with 2,5-PBF, 2,4-PBF showed reduced crystallization capability and comparably satisfactory mechanical proprieties for the intended purpose, while the gas barrier properties were found to be significantly superior and comparable to those of 2,5-PPeF and EVOH [39]. This result was attributed to the different macromolecular structural arrangement of 2,4-PBF compared to 2,5-PBF: it was proposed that the position of the carboxyl groups could make the furan oxygen more sterically available for the formation of interchain interactions, leading to the formation of a more tightly packed partially-ordered mesomorphic phase. In fact, subjecting 2,4-PBF to annealing was shown to worsen its gas barrier properties, since the mesomorph phase was disrupted by the presence of the crystalline phase [39]. The excellent results obtained during the study of 2,4-PBF have opened this line of research to the investigation of the molecular, structural and solid state properties of the other homopolymers belonging to the family of 2,4-poly(alkylene furanoate)s (2,4-PAF), to collect broader information on the structural properties of this new class of polyesters. Therefore, the purpose of the present work was to use the dimethyl ester of 2,4-FDCA to synthesize, compression mold and characterize poly(propylene 2,4-furanoate) (2,4-PPF) from 1,3-propanediol, poly(pentamethylene 2,4-furanoate) (2,4-PPeF) from 1,5-pentanediol and poly(hexamethylene 2,4-furanoate) (2,4-PHF) from 1,6-hexanediol.

2. Experimental section

2.1. Materials

Dimethyl 2,4-furandicarboxylate (2,4-DMF) was synthesized as detailed in the literature [23], then purified to monomer grade with multiple recrystallizations from methanol. The following materials were used as purchased: 1,3-propanediol (PD) (97% purity; Carbosynth Ltd., Combrook, UK); 1,5-pentanediol (PeD) (97% purity; Fluka Chemika GmbH, Buchs, Switzerland); 1,6-hexanediol (HD) (97% purity, Tokyo Chemical Industry Co. Ltd., Tokyo, Japan); 1,4-butanediol (BD) (97% purity) and titanium isopropoxide (TIP) (Sigma-Aldrich, Saint Louis, MO, USA).

2.2. Poly(alkylene furanoate)s Synthesis

The production of poly(alkylene 2,4-furanoate)s (2,4-PTF, 2,4-PPeF, 2,4-PHF) was performed in a 250 mL glass reactor, by the polycondensation method typically used for furan-based polyesters [22]. For all syntheses, 200 ppm of TIP was used as a catalyst and an excess of glycol (300 mol% compared to the ester), both as a reagent and as solvent. The 1st stage of synthesis was the transesterification reaction, which took place under nitrogen flow, at 190 °C, for 120 min, while the 2nd stage was the polymerization reaction, carried out at 210 °C, for 120 min, at a pressure gradually lowered down to 0.05 mbar. During the second step the excess glycol distilled off and the torque increased up to a plateau, at which point the reaction was stopped. The reagents used were 4.0 g (21.9 mmol) of 2,4-DMF and 5.0 g (65.8 mmol) of PD to obtain 2,4-PTF; 3.5 g (19.2 mmol) of 2,4-DMF and 6.0 g (57.6 mmol) of PeD to obtain 2,4-PPeF; 2.9 g (16.0 mmol) of 2,4-DMF and 5.7 g (47.9

mmol) of HD to obtain 2,4-PHF. The synthesized polymers (2,4-PTF, 2,4-PPeF and 2,4-PHF) were purified by dissolving them in hexafluoroisopropanol/chloroform (5% *v*/v) and by precipitating the solution in methanol (1 mL of polymer solution in 10 mL of methanol). After recovery from methanol, the polymers were dried under the fume hood overnight.

2.3. Molecular characterization

The chemical composition of the synthesized polymers was examined using proton nuclear magnetic resonance (^{1}H NMR) spectroscopy on a Varian Inova 400-MHz (Agilent Technologies, Palo Alto, CA, USA) at room temperature. Approximately 10 mg of each polymer were dissolved in 0.7 mL of deuterated chloroform (containing 0.03 *v*/v% of tetramethylsilane as internal standard) and using a few droplets of trifluoroacetic acid, added immediately before the measurements.

To determine the number-average molecular weight (M_n) and the corresponding polydispersity index (Đ) of the synthesized polymers, gel-permeation chromatography (GPC) with a 1525 binary HPLC pump (Waters, Milford, MA, USA) was used, equipped with PLgel 5 mm MiniMIX-C column (Agilent Technologies), at 30 °C. The eluent was GPC-grade chloroform and the flow rate was 1 mL/min. Chloroform solutions with a polymer concentration of 2 mg/mL were prepared, with the addition of a few droplets of hexafluoroisopropanol. To obtain the calibration curve, polystyrene standards were used, in the range of 550–2,500,000 g/mol.

2.4. Film preparation

2.5 g of purified powder of 2,4-PTF, 2,4-PBF, 2,4-PPeF and 2,4-PHF was placed between two sheets of poly(tetrafluoroethylene) (PTFE) and compression molded into 300 μm-thick films with the use of a C12 laboratory press (Carver, Wabash, IN, USA). The compression molding was carried out for 2 min, at a pressure of 9 ton/m^2 and a temperature 30 °C above the T_m of the samples (or the T_g, in the case of the amorphous samples).

2.5. Thermal characterization

To eliminate any possible traces of adsorbed moisture, the samples were compression molded at 150 °C immediately before being subjected to TGA analyses. For TGA analyses, a TGA4000 (PerkinElmer, Waltham, MA, USA), was used to heat 5 mg samples from 40 to 800 °C (10 °C/min), under a flow of 40 mL/min of pure nitrogen. The so-obtained data were used to determine $T_{5\%}$, the temperature at which a weight loss of 5% is achieved, $T_{onset,}$ the temperature at which weight loss begins, and $T_{max,}$ the temperature at which the derivative of the thermogram has reached its minimum value.

DSC analyses were carried out on 5 mg samples, using a DSC6 (PerkinElmer, Waltham, MA, USA). The samples were placed in an aluminum pan, then: 1. heated from −20 to 200 °C at 20 °C/min, 2. cooled from 200 to −20 °C at 100 °C/min, 3. heated from −20 to 200 °C at 20 °C/min. The glass transition temperature (T_g) was obtained considering the intermediate heat flow value between the baselines extending, respectively, from the beginning and the end of the glass-to-rubber transition step. The specific heat variation (ΔC_p) was calculated by considering the height between the two baselines. The melting temperature (T_m) and the enthalpy of fusion (ΔH_m) were obtained by, respectively, the maximum and the total area of the peak of the endothermic phenomenon.

2.6. Structural characterization

Wide-angle X-ray scattering (WAXS) analyses were carried out on film samples, using an X'PertPro diffractometer (PANalytical, Almelo, The Netherlands) equipped with a solid-state X'Celerator detector. X-rays were obtained from a copper source (wavelength of 0,154 nm) and the system moved in steps of 0.1°, with a rate of 100 s/step. Incoherent scattering was not included in the results. By subtracting the amorphous halo from the total area of the diffraction curve, it was possible to obtain the area of the crystalline reflections (A_c). Diving A_c by the total area of the diffraction curve (A_t), the crystallinity index (X_c) was obtained.

Polarized light optical microscopy (PLOM) experiments were carried out with an Axioskop 2 microscope (Carl Zeiss, Oberkochen, Germany), equipped with an Axio Cam ICc 1 (Carl Zeiss, Oberkochen, Germany), a 64,625 HLX 100 W – 12 V halogen optic lamp (Osram, Munich, Germany) and a TMS 94 temperature control system (Linkam Scientific Instruments, Epsom, UK). Samples were observed at room temperature and during a temperature scan up to 200 °C, at a heating rate of 20 °C/min.

2.7. Mechanical characterization

Film samples were subjected to tensile tests with the use of an Instron 5966 (Instron, Norwood, MA, USA) with a transducer-coupled 1 kN load cell. Samples were prepared with 5 mm of width, and 50 mm of height, and the average thickness of each was measured using a micrometer (around 300 μm). They were secured on the grips at a gauge length of 2.0 cm, then they were stretched at a constant rate of 10 mm/min. The results were automatically converted into stress-strain curves and the elastic modulus (E) was obtained as the slope of the initial points of the curve, in a range with linear regression equal to at least 0.99. At least five tests for each material were tested, and the results were reported including their standard deviation.

Cyclical tensile tests were carried out under the same conditions, by stretching until reaching a deformation of 50%, then by removing the stress until reaching 0.005 MPa. 11 cycles of stretching and relaxation were performed, and for each cycle, the hysteresis was calculated as the difference between the integrals of the two curves.

2.8. Gas-barrier properties evaluation

To test the gas barrier properties, a manometric method was used by the Gas Permeability Testing Manual and to the standards ASTM D1434–82(2009) (Standard test method for determining gas permeability properties of plastic film and coating), DIN 53536 (Determination of permeability of rubber to gases) and ISO/DIS 15105–1:2007 (Plastic film and sheeting determination of gas transport rate; part I: differential pressure method). A permeance testing device, type GDP-C (Brugger Feinmechanik GmbH, Munchen, Germany) equipped with an external thermostat HAAKE-Circulator DC10-K15 type (ThermoFisher Scientific, Waltham, MA, USA) was used to test film samples (diameter of at least 10 cm, surface area of 78.5 cm^2) against pure O_2 and CO_2 (pressure = 1 atm, temperature = 23 °C or 38 °C; gas flow = 100 cm^3/min, relative humidity = 0% or 85%). From the pressure-time plot obtained, it was possible to calculate permeability and Gas Transmission Rate (GTR) values. Each measurement was expressed as a mean value, from a triplicate.

3. Results and discussion

3.1. Molecular characterization

The synthesized poly(alkylene 2,4-furanoate)s (Fig. 1) were subjected to ^{1}H NMR analyses. Each group of equivalent hydrogens in the repeating units was labeled with a letter. The spectra and peak assignments are shown in Fig. 2. In all spectra, it is possible to see signals originating from chloroform (7.26 ppm) and the internal standard (tetramethylsilane, 0 ppm). In all samples, the spectra show a pair of singlets around 7–8 ppm, originated from aromatic furan hydrogens, labeled a and b (or a' and b', or a" and b") and located at 8.10 and 7.44 ppm, respectively. At lower chemical shift values it is possible to see the

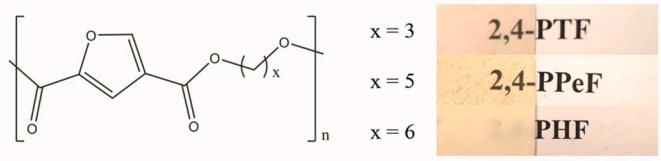

Fig. 1. Poly(alkylene 2,4-furanoate)s chemical structure (left) and compression molded films of poly(trimethylene 2,4-furanoate) (2,4-PTF) (top right), poly (pentamethylene 2,4-furanoate) (2,4-PPeF) (center right), poly(hexamethylene 2,4-furanoate) (2,4-PHF) (bottom right).

signals originated from protons labeled as c and d (or c' and d', or c" and d"), which are the methylene glycol groups closest to the furan subunit. It is important to note that the 2,4 isomer of the furan subunit is not symmetrical and gives rise to two different chemical environments for each ester bond, as already reported in the literature [34,35]. Moreover, the shorter the glycol unit, the greater the influence of the furan subunit on the methylene groups in α position from -COO- moieties: this effect produces a high number of triplet combinations in the case of 2,4-PTF, in the 4.46–4.23 ppm range, making the signals of the methylene groups c and d appear as a group of multiplets. On the contrary, the greater length of the glycol subunit allows us to distinguish two triplets for 2,4-PPeF, at 4.33 and 4.29 ppm (for c' and d' hydrogen, respectively), and two triplets for 2,4-PHF, at 4.32 and 4.27 ppm (for the c" and d" hydrogen, respectively). It is also interesting to note that the signals of the OH-terminated methylene glycol groups are faintly visible in the spectra: they are located at 3.76, 3.67 and 3.65 ppm for 2,4-PTF, 2,4-PPeF and 2,4-PHF, respectively. A situation similar to that discussed for c and d hydrogen can be observed for e hydrogen of 2,4-PTF: this glycol methylene group is influenced at the same time by the furan rings in all of their possible orientations, originating multiplets constituted by superimposed quintuplets, located in the 2.20–1.98 ppm range. In the case of 2,4-PPeF, the corresponding methylene glycol groups are labeled e', and f' and they originate two partly superimposed quintuplets located at 1.81 ppm. The innermost glycol methylene group of 2,4-PPeF is labeled as g' and appears to originate a multiplet located at 1.55 ppm: this signal seems to be influenced by the furan rings in all their possible orientations, similarly to the case of methylene group e of 2,4-PTF. Similarly, in the case of 2,4-PHF, the methylene glycol groups e" and f" originate two partially superimposed quintuplets located at 1.76 ppm and the glycolic g" and h" methylene groups originate a multiplet located at 1.47 ppm. The tiny peak at 1.56 ppm, as also corroborated by the quite broad shape, is due to water. MeOH residue is responsible for the signal at 3.49 ppm. At around 3.65 ppm, the terminal -CH_2OH methylene protons are located. Lastly, the small peaks at 0.86 and 1.26 ppm are due to grease residues.

Overall, ^{1}H NMR results confirm the structure of the synthesized polymers. The success of the synthetic process was further validated by GPC analyses. The results in Table 1 indicate that all polymers had a high number average molecular weight (M_n) and a low polydispersity index (Đ). All polymers had molecular weights above 20 kg/mol, which is typically considered the threshold beyond which a polymer expresses adequate processability and functional properties, making the different GPC results practically irrelevant for comparing the properties of the polyesters under study.

3.2. Thermal characterization

The evaluation of the thermal properties is essential for all polymers, due to their impact on the physical state and stability of materials, both during processing and during use: for this reason, DSC analyses were carried out on compression-molded films of poly(alkylene 2,4-furanoate)s. The results can be found in Table 1. The first transition to

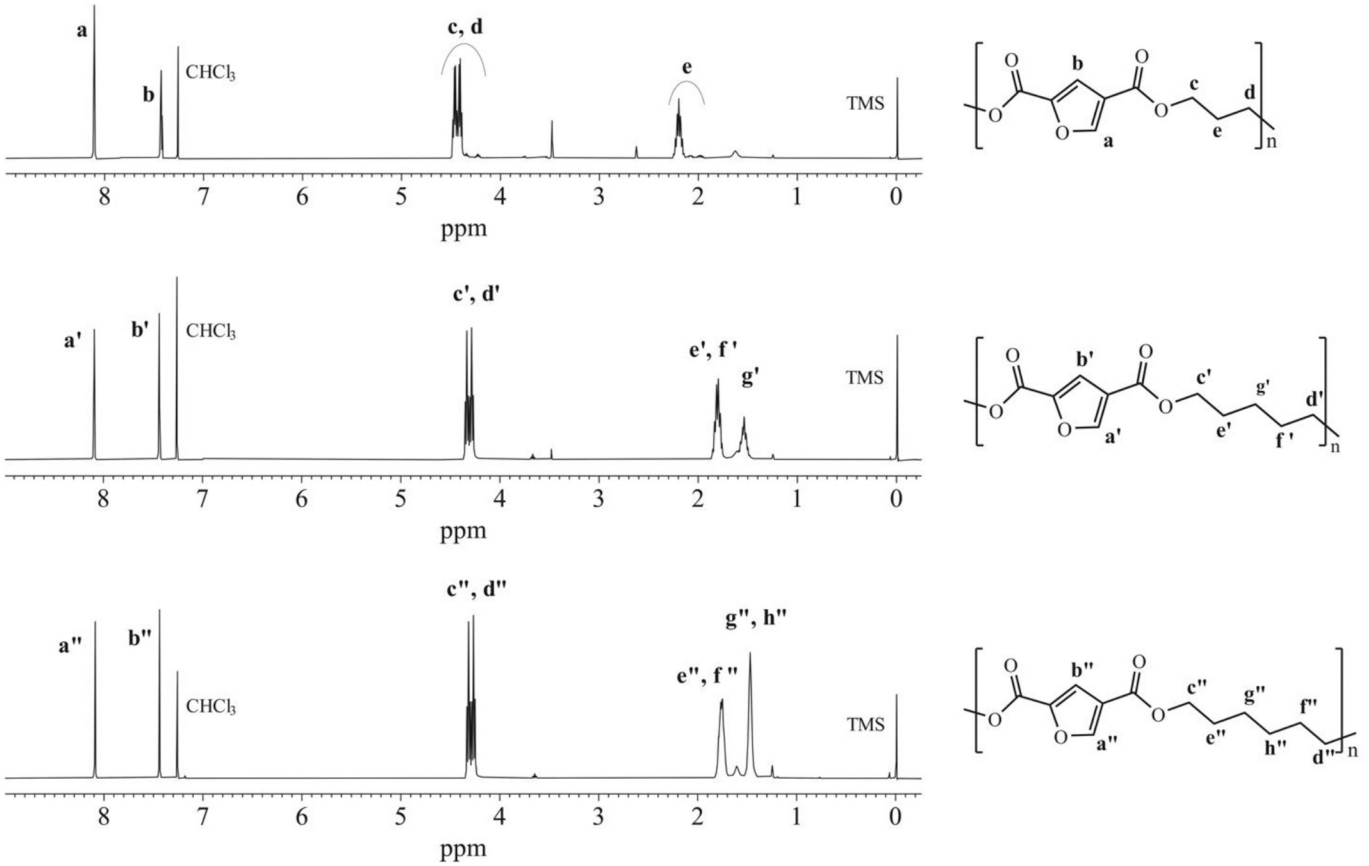

Fig. 2. ^{1}H NMR spectra of 2,4-PTF (top), 2,4-PPeF (middle) and 2,4-PHF (bottom), with peak assignment.

Table 1
GPC, WAXS, DSC (on compression molded films), and TGA data. [a]: cooled in ice after compression molding. [b]: annealed at 45 °C for 24 h. The heating rate is 20 °C/min (R20) unless specified otherwise.

	GPC		DSC				WAXS	TGA		
	M_n kg/mol	Đ	T_g °C	ΔC_p J/(g°C)	T_{endo} °C	ΔH_{endo} J/g	X_c	$T_{5\%}$	T_{onset}	T_{max}
					2,4-PTF					
I scan	31.0	1.9	38	0.394	–	–	0	369	390	409
II scan			44	0.511	–	–	–			
					2,4-PBF [39]					
I scan	44.5	2.3	33	0.376	–	–	0	378	396	409
II scan			33	0.337	–	–	–			
					2,4-PPeF					
I scan	22.7	2.4	11	0.348	–	–	0	356	379	403
II scan			16	0.425	–	–	–			
					2,4-PHF					
I scan R05	44.6	2.0	5	0.271	54	6	13 ± 0.1	374	391	409
I scan R20			9	0.282	58	23				
I scan R40			14	0.295	62	40				
II scan			9	0.471	–	–				
Quenched[a]			6	0.433	–	–	0			
Annealed[b]			9	0.319	60	15	14 ± 0.3			

study was the glass transition temperature (T_g). Across the series of synthesized polyesters, T_g has been shown to follow a clear decreasing trend with the increase in length of the aliphatic subunit. This causes the amorphous component of 2,4-PTF, 2,4-PPeF and 2,4-PHF to be glassy, rubbery and rubbery, respectively, at room temperature. The T_gs of the poly(alkylene 2,5-fuanoate) counterparts with comparable molecular weight have been reported to be higher [22,40] and are compared to the polymers under study in Table 2: the interplay of multiple simultaneous factors could lead to this result, including the flexibility of chains and intermolecular interactions, contributing to higher free volume in the case of poly(alkylene 2,4-furanoate)s. The difference in T_g between the two isomeric forms of each polymer under study becomes progressively smaller as the length of the aliphatic subunit increases: precisely, the difference goes from 14 °C in the case of 2,5-PTF vs 2,4-PTF, down to 4 °C in the case of 2,5-PHF vs 2,4-PHF. This trend can be explained by observing that the density of furan subunits per volume unit decreases as the length of the glycol moiety increases and, as a consequence, the impact of the two furan isomers on the T_g values. In terms of structure, it was observed that 2,4-PTF and 2,4-PPeF films were completely amorphous, while 2,4-PHF showcased an endothermic phenomenon located at 58 °C (Fig. 3, panel A). Upon further investigations, DSC scans carried out at different heating rates revealed a shift towards higher temperatures of the peak position, similarly to what happens for glass transition phenomenon (Table 1 and Fig. 3, panel B). The shift towards higher temperatures is not what would be expected by a traditional crystalline phase, even if it might be explained by superheating and thermal lag. The same type of shift in peak position was consistently observed on the stretched sample (in controlled conditions) and on the 1 year stored film. In order to assess their thermal stability, samples were also subjected to TGA analyses. From the results shown in Table 1 and Fig. S2, the materials were found to be very thermally stable, with a T_{max} up to 409 °C in the case of 2,4-PTF and 2,4-PHF, equal to the T_{max} determined for the 2,4-PBF previously synthesized [39]. 2,4-PPeF was found to have a slightly lower T_{max} of 403 °C, but all samples had higher thermal stability compared to poly(alkylene 2,5-furanoates), especially in the case of 2,4-PTF which, in comparison, had a T_{max} of 23 °C higher than 2,5-PTF [22]. This result can be explained by what has already been suggested in the case of 2,4-PBF [39]: for geometric reasons, the isomerism of poly(alkylene 2,4-furanoate)s might cause the oxygen belonging to the aromatic furan ring to be more sterically accessible for the formation of hydrogen bonds, which could affect the polymer even in its molten state, causing greater resistance to thermal degradation. (See Table 1.)

Table 2
Comparison between the T_g and number average molecular weight of 2,4-poly(alkylene furanoate)s and 2,5-poly(alkylene furanoate)s.

M_n kg/mol	T_g °C	ΔC_p J/(g°C)	M_n kg/mol	T_g °C	ΔC_p J/(g°C)
	2,4-PTF			**2,5-PTF** [22]	
31.0	38	0.394	30.0	52	0.361
	2,4-PBF [39]			**2,5-PBF** [39]	
44.5	33	0.376	32.6	39	0.360
	2,4-PPeF			**2,5-PPeF** [22]	
22.7	11	0.348	29.6	13	0.394
	2,4-PHF			**2,5-PHF** [22]	
44.6	9	0.286	28.9	13	0.205

3.3. Structural characterization

The poly(alkylene 2,4-furanoate)s under study were subjected to wide-angle x-ray diffractometry (WAXS). The so-obtained diffractograms are shown in Fig. 4, panel A and the calculated degree of crystallinity is in Table 1. The WAXS results are in accordance with what was already observed during DSC analyses (Table 1 and Fig. 3, panel A), showing that all the poly(alkylene 2,4-furanoate)s under study are completely amorphous with the exception of 2,4-PHF. In all samples of the series we can see the primary amorphous halo and a secondary, smaller bell at about 10°. A signal such as the latter, wide and at low angles, should indicate the presence of a phase with low degree of order, constituted by chains at high interplanar distance with respect to the crystal lattice. In the case of 2,4-PHF, it is possible to observe the presence of a phase with greater order, indicated by the peaks at $2\theta = 11.7$, 13.7, 19.5, 20.4, 21.3 and 24.8°, which are not as narrow as it would typically be expected by a regular crystalline phase and they are located at different angles than the ones of 2,5-PHF, as shown in Fig. 4, panel B, suggesting a different kind of crystalline cell. Overall, the amorphous halo, the bell at 10°, and the sharper signals of 2,4-PHF can be considered phases at increasingly higher degrees of order. To better understand its structure, 2,4-PHF was subjected to various thermal treatments. First of all, the compression molded film was annealed at 45 °C, for 24 h. The resulting DSC scan (Fig. 3, panel A) shows that its melting temperature moved from 58 °C to 60 °C and the melting peak was narrower, possibly indicating that the less ordered domains were provided with enough energy to rearrange and achieve a greater degree of order. However, the corresponding WAXS diffractogram (Fig. 4, panel B) did not show a clear variation in the peaks of 2,4-PHF. 2,4-PHF was also compression molded a second time and quenched in ice. The resulting material had no crystalline peaks, but only the amorphous halo and the smaller bell at 10° (Fig. 4, panel B).

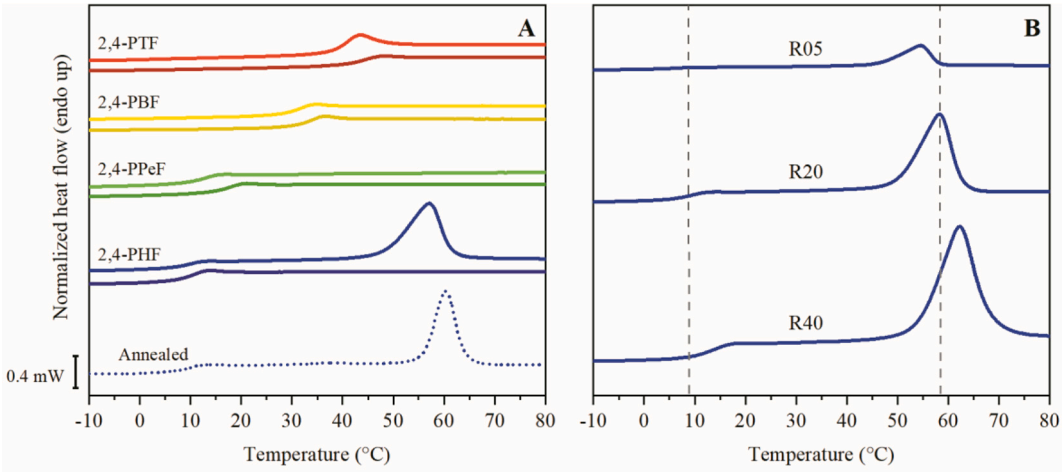

Fig. 3. Panel A: DSC traces of compression molded films: 1st scan on top (light color), 2nd scan at the bottom (dark color); 2,4-PHF annealed for 24 h at 45 °C (dotted line). Panel B: DSC traces of a 2,4-PHF film at various heating rates, R5, R20 and R40, expressed in °C/min. Heat flow normalized on the sample mass (mg).

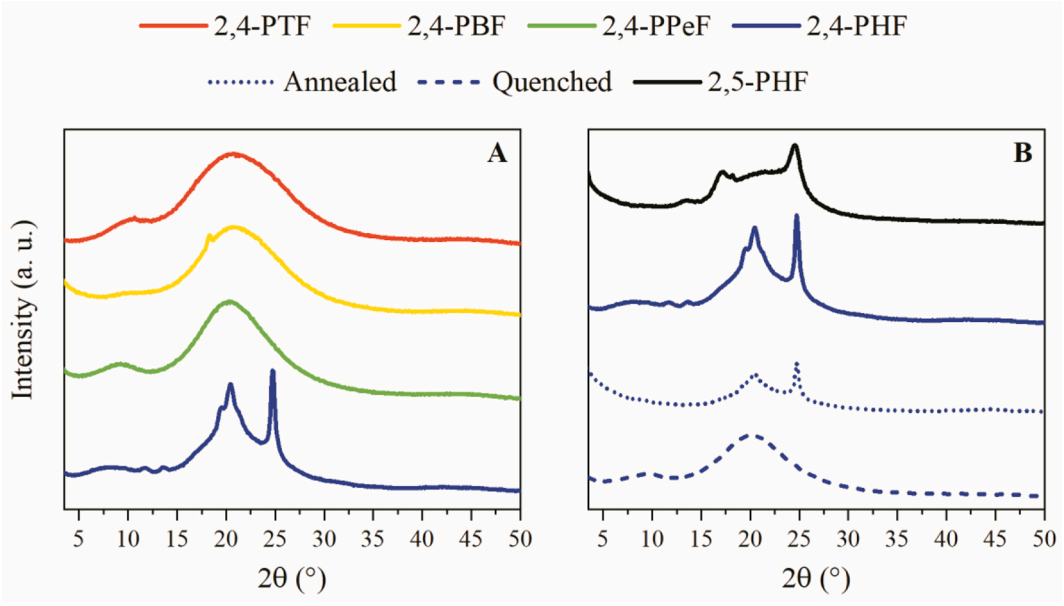

Fig. 4. WAXS patterns of compression molded films. Panel A: 2,4-PTF, 2,4-PBF [39], 2,4-PPeF, 2,4-PHF. Panel B: 2,5-PHF [22] compared to 2,4-PHF subjected to ballistic cooling after compression molding (solid line), annealing at 45 °C for 24 h (dotted line), quenching in ice after compression molding (dashed line).

To gather more information on their structure, polarized light optical microscopy was carried out on the samples under study. The films were observed both at room temperature and on a temperature heating scan. A selection of pictures is shown in Fig. 5 and Fig. S3. In the case of 2,4-PTF, 2,4-PPeF, and 2,4-PBF (previously synthesized [39]), the texture of the samples was not completely transparent, as expected for amorphous polymers, remaining almost unchanged even at temperatures much higher than their T_gs (200 °C) (Fig. S3). The most interesting finding involved 2,4-PHF: in this case, the sample showed some interaction with polarized light, which increased with the increase in temperature. Once at 200 °C, the sample holder was compressed, showing patterns reminiscent of a liquid-crystalline *schlieren* texture, already observed for other polyesters in the literature [41–47]. After compression, the material would return to its molten, transparent state. This was interpreted as potential evidence of the development of a mesophase: in fact, it is possible that intermolecular interactions could form even after the isotropization temperature of 2,4-PHF, originating a reversible birefringence phenomenon as a consequence of the compression of the sample. This hypothesis is confirmed by the literature, since the formation of a mesophase of furan-based polyesters has been reported to be favored by compression molding. In fact, the compression of furan-based polymers might lead to the rearrangement of the furanic rings in a preferential orientation which facilitates the formation of a larger number of intermolecular C– H···O bonds [40].

3.4. Mechanical properties

The series of poly(alkylene 2,4-furanoate)s, including the previously synthesized and studied 2,4-PBF [39], was found to have mechanical properties tunable by changing the length of the glycolic subunit, similarly to their 2,5-isomeric counterparts [22] (Table 3). Specifically, poly(alkylene 2,4-furanoate)s showcased a full range of mechanical behaviors correlated to their physical state (Fig. 6, panel A): the glassy and amorphous 2,4-PTF was rigid, the partially-ordered 2,4-PHF had a yield point and was flexible and tough, and finally the amorphous and rubbery 2,4-PPeF had the stress-strain response typical of a thermoplastic elastomer, with low elastic modulus and high elongation at break. For further demonstrating the elastomeric properties of 2,4-PPeF,

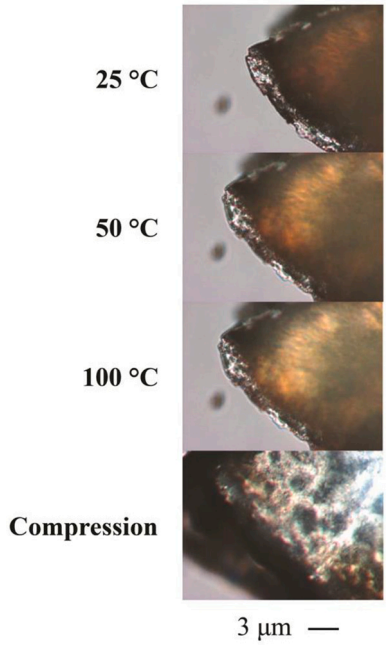

Fig. 5. Polarized optical microscopy pictures taken on a film sample of 2,4-PHF. From top to bottom: 25 °C, 50 °C, 100 °C and compression of the film at 100 °C.

Table 3
Mechanical characterization data.

	2,4-PTF	2,4-PBF	2,4-PPeF	2,4-PHF	PET [48]
E (MPa)	1428 ± 146	939 ± 72	4 ± 1	110 ± 21	3100
σ_y (MPa)	–	16 ± 1	–	7 ± 1	–
ε_y (%)	–	4 ± 1	–	19 ± 2	–
σ_b (MPa)	38 ± 2	16 ± 6	4 ± 1	24 ± 6	58
ε_b (%)	4 ± 1	564 ± 139	949 ± 198	851 ± 36	50

it was possible to subject it to cyclic tensile tests (Fig. 6, panel B): the samples had low hysteresis values starting from the second cycle (Fig. 6, panel C), which is a desirable result, since it resembles the behavior of an ideal elastomer. Moreover, 2,4-PPeF showcased a noticeable elastic recovery of its initial shape after break (Video S1) and interestingly, also 2,4-PHF expressed elastic recovery after break (Video S2). As already shown in this work, 2,4-PPeF is an amorphous and rubbery polymer at room temperature. Polymers showcasing these structural characteristics do not typically have an elastomeric behavior, however, the presence of a mesomorph phase was confirmed experimentally in a polymer very similar to 2,4-PPeF: its isomer, 2,5-PPeF [40]. This polymer chains arrangement arises from H-bond like interactions and π-π bonds that can lead to mono- or bi-dimensional order (mesophase). Mesomorph phases are particularly challenging to identify during DSC or WAXS studies, but even when the order is not high enough to produce a certain periodicity, the underlying interactions are still present. The H-bond like interactions and π- π bonds could be responsible for the unusual processability of polymers like 2,4-PPeF and could act as a physical crosslink, causing a behavior similar to the one of a thermoplastic elastomer. The presence of chemical crosslinks can be excluded because of the unchanged processability and solubility of 2,4-PPeF films after subjecting them to mechanical tests. Comparing the mechanical properties of all poly(alkylene 2,4-furanoate)s, it can be noted that the elastic modulus is the highest for 2,4-PTF, slightly lower for 2,4-PBF, intermediate for 2,4-PHF and the lowest for 2,4-PPeF. Conversely, the elongation at break is the highest for 2,4-PPeF, slightly lower for 2,4-PHF, intermediate for 2,4-PBF and the lowest for 2,4-PTF. These observations are predictable, considering that the trend of decreasing modulus is parallel to the increase of the glycolic chain length, while 2,4-PHF shows an increase due to its semicrystalline state. Also, the different elongation at break can be explained considering that 2,4-PHF has a partially ordered phase which requires energy to disrupt, increasing the toughness of the material, while 2,4-PBF is completely amorphous. It is interesting to compare the mechanical properties of the two isomeric families of homopolymers: 2,4-PTF had the same modulus, but was slightly more ductile than 2,5-PTF, which was reported to have modulus of 1341 MPa and elongation at break of 3% [22]. 2,4-PBF, had a slightly lower modulus but even higher ductility than 2,5-PBF, which was reported to have a modulus of 1290 MPa and elongation at break of 157% [22]. 2,4-PPeF showed very similar results when compared to 2,5-PPeF, which was reported to have a modulus of 9 MPa and elongation at break of 1050% [22]. Finally, 2,4-PHF showed mechanical properties that were considerably superior to the ones of its isomeric counterpart 2,5-PHF, which was reported to have a modulus of 906 MPa and elongation at break of 42% [22].

3.5. Gas barrier properties

The gas barrier properties of a polymer film used in the field of food packaging are fundamental to guarantee the shelf-life of food products, preventing alterations of the modified-atmosphere packaging, oxidation, and losses of carbon dioxide from carbonated beverages. For this reason, the gas barrier properties of the polymers under study were tested towards O_2 and CO_2, both in dry (0% relative humidity) and humid (85% relative humidity) atmospheres (Table 4 and Fig. 7, panel A). The comparison with commercial polymers used in the field of food packaging showed remarkable results for all the poly(alkylene 2,4-furanoate) homopolymers under study (Fig. 7, panel C). Compared to PET, both 2,4-PHF and 2,4-PTF showed lower CO_2 transmission rates, while 2,4-PBF and 2,4-PPeF were found to have vastly improved gas barrier properties, (by approximately two orders in magnitude), comparable to those of poly(ethylene vinyl alcohol) (EVOH), the industry standard for excellent gas barrier properties in polymeric food packaging materials. The barrier improvement factor with respect to PET [49] (O_2-BIF and CO_2-BIF), at 23 °C and 0% RH, was calculated for all the 2,4-poly(alkylene furanoate)s under study, since PET is currently the most industrially produced polyester for food packaging applications. The results confirm that the gas barrier properties of 2,4-PHF are very similar to the ones of PET (O_2-BIF = 1; CO_2-BIF = 2), 2,4-PTF had superior gas barrier properties than PET (O_2-BIF = 3; CO_2-BIF = 18), 2,4-PPeF had vastly improved gas barrier properties (O_2-BIF = 120; CO_2-BIF = 291) and 2,4-PBF had the best gas barrier properties (O_2-BIF = 164; CO_2-BIF = 527).

Compared to poly(alkylene 2,5-furanoate)s, the polymers under study showed similar gas barrier properties, except for 2,4-PTF and 2,4-PBF (Fig. 7, panel B). In particular, in the case of 2,4-PBF, the gas transmission rates decreased by two orders of magnitude, evidencing a much higher gas blocking ability in comparison to 2,5-PBF, and the possible causes of this behavior were discussed in the literature: in particular, the excellent performance of 2,4-PBF was found to be related to its amorphous state and lower crystallization capacity, which was hypothesized to optimize the formation of a partially ordered mesomorph phase [39]. The formation of a mesomorph phase has been shown [40] or hypothesized for 2,5-PAF and 2,4-PAF polymers, and the lower mobility of the 2,4-PAF chains, proven in other studies [32,33] might be sufficient to explain this. As further evidence of the importance of the amorphous state, even amorphous 2,5-PBF was found to show greater gas barrier properties in comparison to semi-crystalline 2,5-PBF and semi-crystalline 2,4-PBF [39]. 2,4-PPeF and 2,4-PHF were found to have slightly higher permeability when compared with their isomeric counterparts, and this could be explained by the fact that their T_g is lower (Table 2), which causes an increase in free volume at room temperature, making their amorphous phase more permeable to gases. Likewise, a decrease in gas barrier properties could be observed for 2,4-PTF, when compared to 2,5-PTF: both polymers are glassy at room temperature,

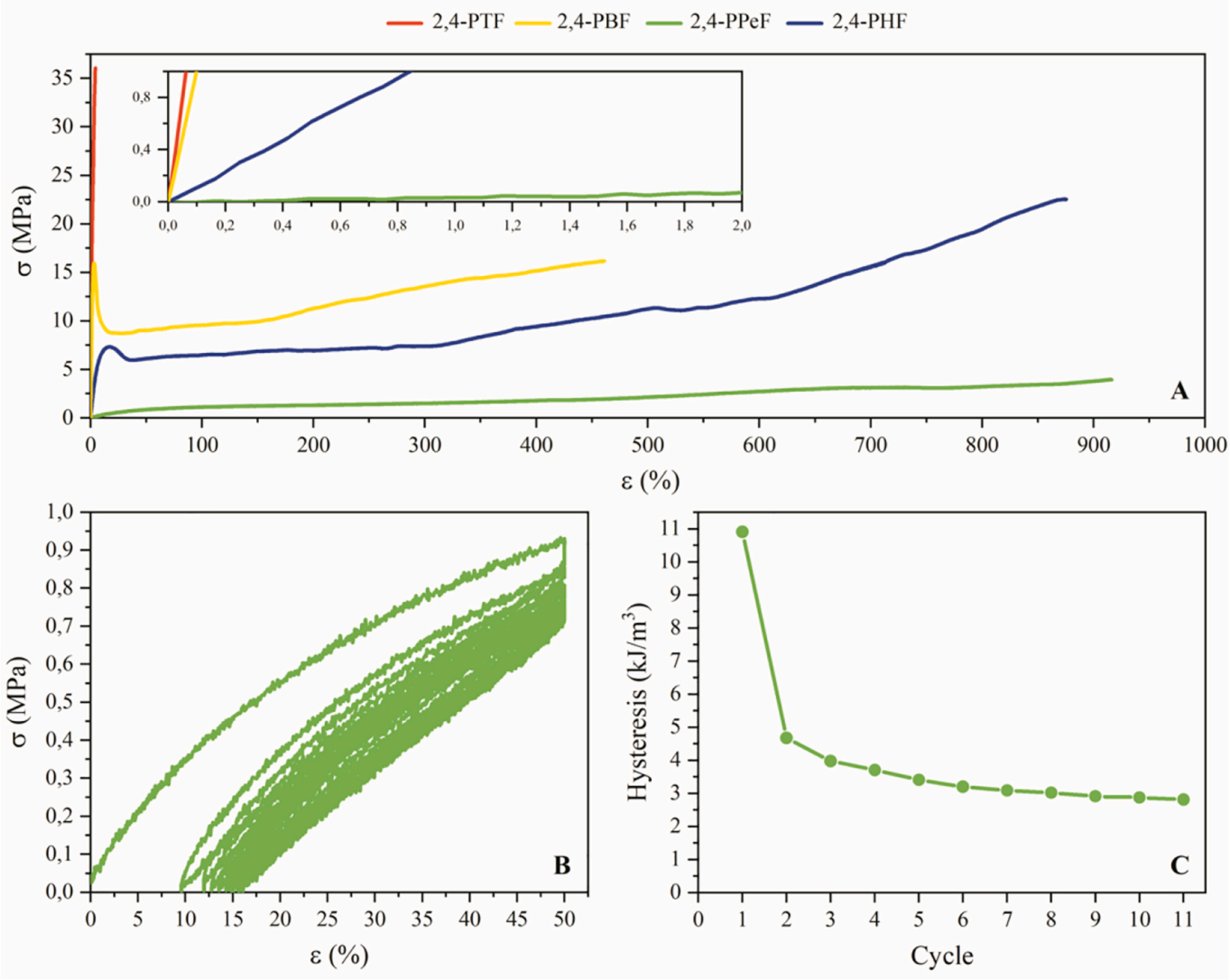

Fig. 6. Panel A: Stress-strain curves for 2,4-PTF, 2,4-PBF [39], 2,4-PPeF, 2,4-PHF. Inset: magnification at low elongation. Panel B: Cyclic stress-strain curves for 2,4-PPeF. Panel C: Hysteresis values for each cycle represented in panel B.

Table 4
O_2 and CO_2 transmission rates for the compression-molded films of 2,4-PTF, 2,4-PBF [39], 2,4-PPeF, 2,4-PHF, expressed in (cm^3 cm)/(m^2 day atm), under a variety of humidity and temperature conditions. The shelf life of flexible film for fresh food products and of rigid bottles for carbonated drinks is estimated as shown in the literature [50].

			2,4-PTF	2,4-PBF	2,4-PPeF	2,4-PHF
Gas transmission rates						
O_2-TR	23 °C	0% RH	0.1380	0.0022	0.0030	0.3836
O_2-TR	23 °C	85% RH	0.0781	0.0026	0.0047	0.6401
CO_2-TR	23 °C	0% RH	0.1225	0.0007	0.0031	0.4432
CO_2-TR	23 °C	85% RH	0.0732	0.0021	0.0031	0.4954
O_2-TR	38 °C	0% RH	0.0124	–	–	–
CO_2-TR	38 °C	0% RH	0.0101	–	–	–
Shelf life						
Bottle for carbonated drink (days)			691	24,089	–	–
vs biaxially oriented PET			+297%	+13,744%	–	–
Flexible film for fresh food (days)			–	–	35	< 1
vs PVC wrap film			–	–	+8436%	Comparable

and this might lead to an inferior optimization of interchain hydrogen bonds, which are essential for the formation of a furanic mesophase, highly impermeable to gases [40]. However, in the case of 2,4-PTF, the T_g is lower, close to room temperature, so we could assume that the glass might have higher free volume, facilitating the passage of gas, and still not enough mobility for the macromolecular chains to optimize their conformation and intermolecular interactions. To validate this hypothesis, in the specific case of 2,4-PTF, gas barrier tests were carried out again at 38 °C, a temperature corresponding to the T_g of the polymer. The transition from the glassy to rubbery state increases the free volume, worsening the gas-barrier properties, but it should also unlock the movement of the furan macromolecules, improving the gas-block capacity. The results (Table 4) illustrate that the latter effect prevails over the increase in free volume, determining a remarkable decrease in gas transmission rates, by an order of magnitude, confirming that the optimization of intermolecular interactions is crucial to obtain excellent gas barrier properties in furan-based polyesters. Moreover, 2,4-PTF was left to rest for two weeks and the gas barrier tests were repeated at 23 °C: the results coincided with those obtained before the tests at 38 °C, confirming that the improvements obtained were reversible, exclusively due to the optimization of the H-bonds, caused by the temperature at which the tests were carried out. This behavior is corroborated even further by observing the gas transmission rate values obtained in humid conditions

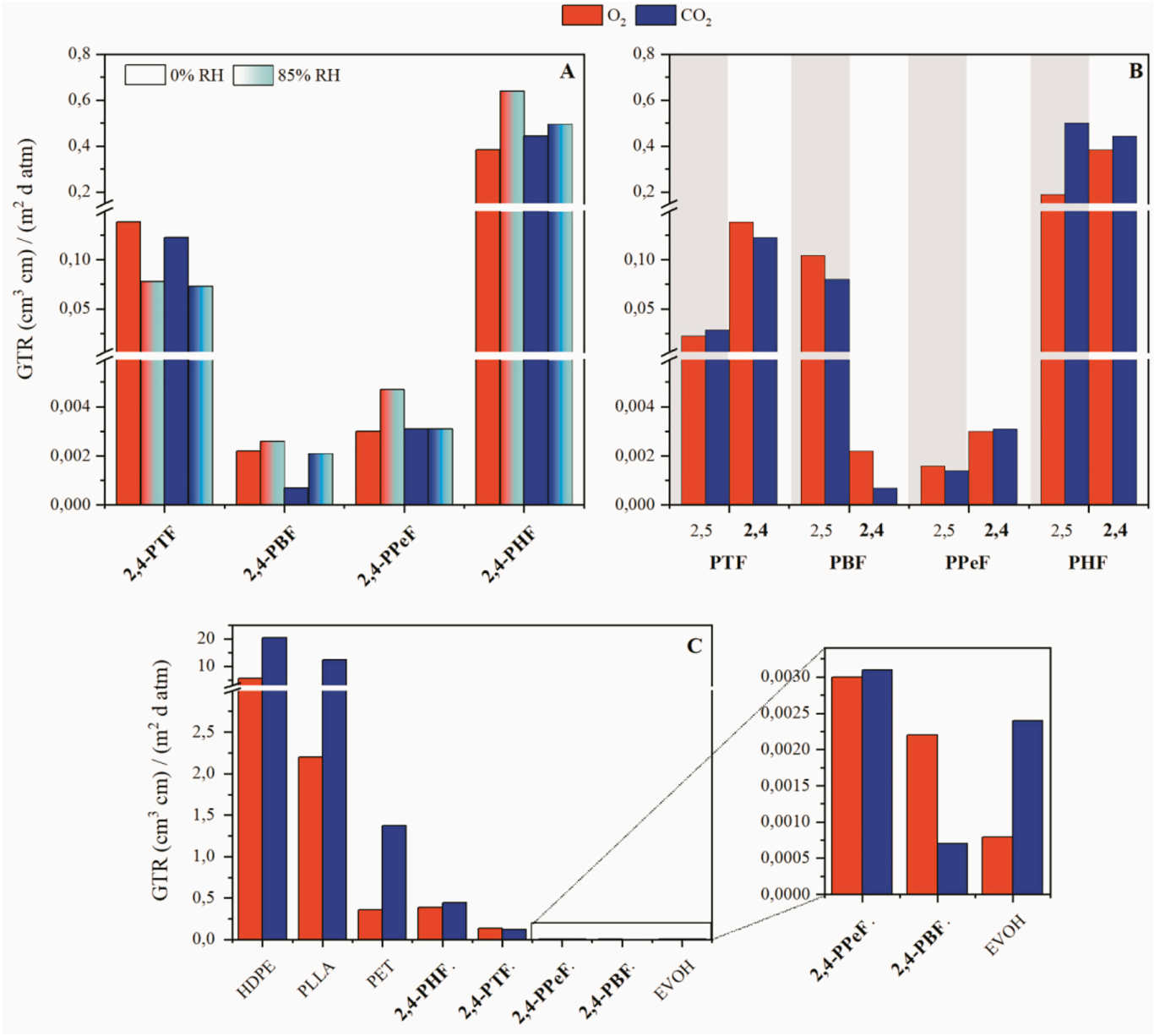

Fig. 7. O_2 and CO_2 transmission rates at 23 °C in dry (0% RH) conditions. Panel A: values for 2,4-PTF, 2,4-PBF [39], 2,4-PPeF, 2,4-PHF, also in humid (85% RH) conditions. Panel B: values for 2,4-PAF respectively compared to 2,5-PTF [22], 2,5-PBF [22], 2,5-PPeF [22], 2,5-PHF [22]. Panel C: values for 2,4-PAF compared to HDPE [50], PLLA [50], PET [49], EVOH (32% ethylene) [50]. Inset: magnification at low GTR.

(Fig. 7, panel A) follow a different trend in the case of 2,4-PTF, when compared to the other poly(alkylene 2,4-furanoate)s: in particular, an increase in gas transmission rate is observed in the case of 2,4-PBF, 2,4-PPeF and 2,4-PHF, possibly because the plasticizing effect of water has prevailed over its crosslinking effect, causing an increase in free volume and an increase in gas passage. Although, in the case of 2,4-PTF, the plasticization of the material may have allowed the otherwise glassy chains to be mobile enough to optimize their intermolecular bonds, leading to less gas passage, similar to what was discussed in the case of tests carried out at 38 °C. For the other polymers under study, the gas barrier properties in humid conditions lead to relatively small changes in gas barrier properties, highlighting the outstanding performance of poly (alkylene 2,4-furanoate)s, which were found to be by far superior to EVOH not only in terms of mechanical properties, but also because they can maintain their excellent gas barrier properties in humid conditions, making their use in single-layer packaging applications possible.

As a way to compare the potential performance of the materials under study, the shelf life was estimated as shown in the literature [50], and showcased in Table 4. The results are a theoretical estimate which concretely shows the potential consequences of the outstanding gas barrier properties of 2,4-PAF. For 2,4-PTF and 2,4-PBF, the primary application in food packaging is predicted to be rigid packaging due to their high elastic modulus, so the case considered was of a single-material bottle 0.055 cm thick, with a surface area of 0.14 m^2, containing 1 L of carbonated liquid with a CO_2 concentration of 3500 ppm and an internal pressure of 2.75 atm, stored at 23 °C. Given the CO_2-TR obtained in humid conditions (Table 4), a CO_2 loss higher than 20% determines the shelf life of the beverage [50], which was calculated to be exceptionally high for 2,4-PTF and 2,4-PBF (Table 4). These results might be further improved after the potential processing via blow molding, which typically induces biaxial orientation in similar polymers, such as PET, further enhancing their gas barrier properties. Biaxially oriented films should be produced and tested in the future to confirm this hypothesis. In comparison, the shelf life of a biaxially

oriented PET bottle, calculated in the same manner and using a CO_2-TR found in the literature [51], was estimated to be equal to 174 days, a much lower value compared to 2,4-PTF and 2,4-PBF, which had a shelf life equal to 691 and 24,089 days, respectively (Table 4). On the other hand, for 2,4-PPeF and 2,4-PHF, the primary application in food packaging is predicted to be flexible films, due to the lower elastic modulus, so the case considered was of a mono-material film 0.005 cm thick, with a surface area of 0.10 m^2, containing 200 g of fresh food products, such as meat, dairy or vegetables, stored at 23 °C. Given the O_2-TR obtained under humid conditions (Table 4), an input of O_2 higher than 5 ppm determines the shelf life of the product [50]. In comparison, the O_2-TR found in the literature [51] for PVC kitchen wrap films was used to estimate the shelf life in analogous conditions, which was discovered to be inferior to 1 day, comparably to 2,4-PHF, while 2,4-PPeF was associated with a significantly longer shelf life, 35 times higher than that of PVC (Table 4).

In summary, the study of the gas barrier properties of 2,4-PAF showed that:

- In comparison with their respective 2,5-PAF isomers, 2,4-PBF showed vastly improved gas barrier, previously attributed to its amorphous state, its geometry and chain mobility [32,33,39]. 2,4-PPeF and 2,4-PHF had slightly higher permeability because of their lower T_g. The permeability was further increased for 2,4-PTF because of its glassy state, as demonstrated with gas barrier experiments carried out above T_g.
- In humid conditions, the permeability increased for 2,4-PBF, 2,4-PPeF and 2,4-PHF, possibly because the plasticizing effect of water, while in 2,4-PTF, the same plasticization effect caused lower permeability, since it might have favored intermolecular bond formation.
- In comparison with commercial products, 2,4-PHF and 2,4-PTF had lower CO_2 permeability than PET, while 2,4-PBF and 2,4-PPeF had outstanding gas barrier properties, comparable to those of EVOH. In substitution to PVC wrap films, 2,4-PPeF was estimated to cause an increase of shelf life of about 35 days, while in comparison to PET bottles, 2,4-PBF was estimated to cause an increase of shelf life of >65 years.

3.6. Self-healing microstructure of 2,4-PHF

While analyzing 2,4-PHF, several interesting details were observed. As previously mentioned, DSC experiments carried out on 2,4-PHF at various heating rates showed that the peak at 58 °C shifted towards higher temperatures, unlike the typical melting of a crystalline phase (Fig. 3, panel B). Additionally, PLOM experiments carried out on 2,4-PHF at 200 °C showed that, upon compression, the material interacted with the polarized light to produce patterns reminiscent of a liquid-crystalline schlieren texture (Fig. 5), and interestingly, the formation of a partially-ordered phase in 2,5-PAF homopolymers was also observed to be favored by compression [40]. More evidence of an unusual behavior of 2,4-PHF was gathered after subjecting the sample to tensile tests: specifically, the initially opaque samples of 2,4-PHF (Fig. 1) became more transparent after stretching (Fig. 8). This was an unexpected result, since the typical effect of tensile tests on semi-crystalline polymers is the strain-induced crystallization of the material, which leads to a more opaque sample. The decreased thickness as a consequence of the plastic deformation could have been a factor contributing to the increased transparency of 2,4-PHF, but this could not be considered the only cause: upon further investigation, both DSC and WAXS analyses were carried out on the stretched samples at various times after the tensile tests (Fig. 9; Table 5), showing that the melting enthalpy and the degree of crystallinity decreased considerably immediately after stretching, then they slowly recovered over time, reaching the pristine melting enthalpy (the one the material had before stretching) after a year of storage at room temperature. Additionally, the melting peak of

Fig. 8. Difference in transparency between the non-stretched (left) and stretched (right) area of a 2,4-PHF sample, 1 min after stretching the sample until break.

2,4-PHF also changed in position, from 58 to 48 °C immediately after stretching, then the peak slowly shifted towards higher temperatures, reaching a melting temperature of 53 °C after a year of storage. Moreover, despite being partially ordered, the deformation past the yield point on 2,4-PHF was found to be reversible over time, as observed by its shape recovery behavior (Video S2). Finally, despite the presence of an ordered phase on both 2,5-PHF and 2,4-PHF, the latter has much higher toughness (5 vs 114 J/m^3, respectively). The large amount of evidence presented suggests the presence of a self-healing microstructure, possibly originated by hydrogen bond interactions which lead to the formation of a partially ordered 2D phase, already observed in the past for 2,5-PAF [40] and inferred in the case of 2,4-PBF [39]. More sophisticated experimental techniques which are out of the scope of this work will be necessary to provide definitive proof of this hypothesis.

4. Conclusions

In the present work it was possible to successfully achieve the synthesis and compression molding of 2,4-PAF, a family of homopolymers based on 2,4-FDCA, a structural isomer of the better known 2,5-FDCA, and linear glycols of increasing chain length, evaluating their performance in food packaging applications. ^{1}H NMR and GPC analyses confirmed the success of the synthetic process. DSC analyses showed a decreasing trend of T_g values with increasing glycol chain length. TGA analyses showed high thermal stability for all the homopolymers under study, with T_{max} higher than 400 °C. Tensile tests showed a wide range of mechanical response, from the stiff 2,4-PTF and 2,4-PBF, suitable for rigid packaging applications, to the flexible and tougher 2,4-PHF and finally 2,4-PPeF, which presented the stress-strain response typical of a thermoplastic elastomer, with low hysteresis during cyclical tests. Both 2,4-PPeF and 2,4-PHF showed shape recovery after breaking, which makes them suitable for the production of flexible and elastic packaging. Gas barrier tests showed that 2,4-PBF and 2,4-PPeF had gas transmission rates comparable to those of poly(ethylene vinyl alcohol) (EVOH), the industrial standard for excellent gas barrier properties in polymeric materials for food packaging, but unlike EVOH, the gas barrier values remained practically unchanged in humid conditions and were paired with excellent mechanical properties. When used for the production of carbonated beverages, 2,4-PTF and 2,4-PBF would provide an exceptional increase in shelf life, particularly in the case of 2,4-PBF, which would virtually stop the loss of CO_2. When used for the production of flexible films for fresh food products, compared to PVC wrap films, 2,4-PHF would have similar performance, while 2,4-PPeF would improve the shelf life by >8000%, greatly supporting the prevention of food loss and food waste. Finally, an in-depth characterization of 2,4-PHF through mechanical, thermal, and optical microscopy analyses lead to the conclusion that a partially ordered self-healing phase might have caused the unusual behavior of the material. Overall, the results open new possibilities for investigation in the field of Materials Physics and highlight the great potential of 2,4-PAFs as a new class of polyesters for the production of biobased, monolayer, easily recyclable, and sustainable food packaging applications.

Supplementary data to this article can be found online at https://doi.org/10.1016/j.reactfunctpolym.2024.106010.

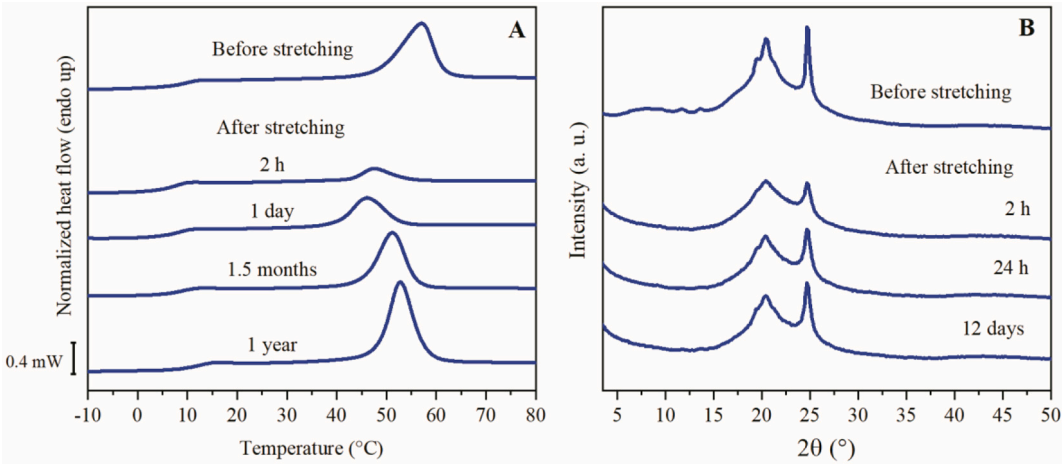

Fig. 9. DSC (Panel A) and WAXS (Panel B, equatorial beam incidence) traces of a 2,4-PHF film, before and at various intervals after stretching. Heat flow normalized on the sample mass (mg).

Table 5
Chronological series of DSC (I scan) and WAXS (equatorial beam incidence) data on stretched 2,4-PHF films. [a] Time elapsed from the end of the stress-strain test.

		DSC				WAXS
	Time[a]	T_g °C	ΔC_p J/(g°C)	T_{endo} °C	ΔH_{endo} J/g	X_c
Not stretched	–	9	0.286	58	18	13 ± 0.1
Stretched	2 h	6	0.347	48	4	8 ± 0.3
Stretched	24 h	7	0.311	46	10	11 ± 1
Stretched	48 h	–	–	–	–	11 ± 0.3
Stretched	5 days	–	–	–	–	11 ± 0.2
Stretched	12 days	–	–	–	–	12 ± 0.9
Stretched	26 days	–	–	–	–	12 ± 1.8
Stretched	45 days	8	0.280	51	16	–
Stretched	1 year	12	0.374	53	21	–

CRediT authorship contribution statement

Enrico Bianchi: Writing – review & editing, Writing – original draft, Software, Methodology, Investigation, Formal analysis, Data curation. **Michelina Soccio:** Writing – review & editing, Writing – original draft, Validation, Supervision, Project administration, Methodology, Investigation, Funding acquisition, Data curation, Conceptualization. **Valentina Siracusa:** Writing – review & editing, Validation, Software, Formal analysis, Data curation. **Massimo Gazzano:** Writing – review & editing, Validation, Software, Investigation, Formal analysis, Data curation. **Shanmugam Thiyagarajan:** Writing – review & editing, Methodology, Investigation, Formal analysis. **Nadia Lotti:** Writing – review & editing, Validation, Supervision, Project administration, Funding acquisition, Conceptualization.

Declaration of competing interest

The authors declare that they have no known competing financial interests or personal relationships that could have appeared to influence the work reported in this paper.

Data availability

Data will be made available on request.

Acknowledgments

E.B., M.S., N.L., acknowledge the Italian Ministry of University and Research.

References

[1] PlasticsEurope, Plastics – the Facts. https://plasticseurope.org/knowledge-hub/plastics-the-facts-2022/, 2022.
[2] S. Sharma, S. Chatterjee, Microplastic pollution, a threat to marine ecosystem and human health: a short review, Environ. Sci. Pollut. Res. 24 (2017) 21530–21547, https://doi.org/10.1007/s11356-017-9910-8.
[3] C.J. Moore, Synthetic polymers in the marine environment: a rapidly increasing, long-term threat, Environ. Res. 108 (2008) 131–139, https://doi.org/10.1016/j.envres.2008.07.025.
[4] Introduction, in: J.R. Wagner, S.B. Marks, J.R.B.T.-M.F.P, Second E. Wagner (Eds.), Multilayer Flex. Packag, Second Edi, Elsevier, 2016, pp. 3–13, https://doi.org/10.1016/B978-0-323-37100-1.00001-6.
[5] S. Ebnesajjad (Ed.), Plastic Films in Food Packaging, William Andrew Publishing, Oxford, 2013, https://doi.org/10.1016/B978-1-4557-3112-1.00018-1.
[6] R.E.J. Schnurr, V. Alboiu, M. Chaudhary, R.A. Corbett, M.E. Quanz, K. Sankar, H. S. Srain, V. Thavarajah, D. Xanthos, T.R. Walker, Reducing marine pollution from single-use plastics (SUPs): a review, Mar. Pollut. Bull. 137 (2018) 157–171, https://doi.org/10.1016/j.marpolbul.2018.10.001.
[7] D. Xanthos, T.R. Walker, International policies to reduce plastic marine pollution from single-use plastics (plastic bags and microbeads): a review, Mar. Pollut. Bull. 118 (2017) 17–26, https://doi.org/10.1016/j.marpolbul.2017.02.048.
[8] M. Weiss, J. Haufe, M. Carus, M. Brandão, S. Bringezu, B. Hermann, M.K. Patel, A review of the environmental impacts of biobased materials, J. Ind. Ecol. 16 (2012) S169–S181, https://doi.org/10.1111/j.1530-9290.2012.00468.x.
[9] P. Ning, G. Yang, L. Hu, J. Sun, L. Shi, Y. Zhou, Z. Wang, J. Yang, Recent advances in the valorization of plant biomass, Biotechnol. Biofuels 14 (2021) 102, https://doi.org/10.1186/s13068-021-01949-3.
[10] T. Werpy, G. Petersen, A. Aden, J. Bozell, J. Holladay, J. White, A. Manheim, E.D. L. Lasure, S. Jones, M. Gerber, K. Ibsen, L. Lumberg, S. Kelley, Top Value Added Chemicals from Biomass - Results of Screening for Potential Candidates from Sugars and Synthesis Gas, U.S. Department of Energy, 2004.
[11] J.J. Bozell, G.R. Petersen, Technology development for the production of biobased products from biorefinery carbohydrates—the US Department of Energy's "top 10" revisited, Green Chem. 12 (2010) 539, https://doi.org/10.1039/b922014c.
[12] E. de Jong, H. Roy, A. Visser, A.S. Dias, C. Harvey, G.-J.M. Gruter, The road to bring FDCA and PEF to the market, Polymers (Basel). 14 (2022) 943, https://doi.org/10.3390/polym14050943.
[13] A. Scott, DuPont, ADM eye biobased polyester, C & EN Glob. Enterp. 94 (2016), https://doi.org/10.1021/cen-09404-notw2.
[14] J.-G. Wang, X.-Q. Liu, J. Zhu, From furan to high quality bio-based poly(ethylene furandicarboxylate), Chin. J. Polym. Sci. 36 (2018) 720–727, https://doi.org/10.1007/s10118-018-2092-0.
[15] X. Fei, J. Wang, J. Zhu, X. Wang, X. Liu, Biobased poly (ethylene 2,5-furancoate): no longer an alternative, but an irreplaceable polyester in the polymer industry, ACS Sustain. Chem. Eng. 8 (2020) 8471–8485, https://doi.org/10.1021/acssuschemeng.0c01862.
[16] D.G. Papageorgiou, I. Tsetsou, R.O. Ioannidis, G.N. Nikolaidis, S. Exarhopoulos, N. Kasmi, D.N. Bikiaris, D.S. Achilias, G.Z. Papageorgiou, A new era in engineering plastics: compatibility and perspectives of sustainable Alipharomatic poly(ethylene terephthalate)/poly(ethylene 2,5-furandicarboxylate) blends, Polymers (Basel). 13 (2021) 1070, https://doi.org/10.3390/polym13071070.
[17] K. Loos, R. Zhang, I. Pereira, B. Agostinho, H. Hu, D. Maniar, N. Sbirrazzuoli, A.J. D. Silvestre, N. Guigo, A.F. Sousa, A perspective on PEF synthesis, properties, and end-life, Front. Chem. 8 (2020) 585, https://doi.org/10.3389/fchem.2020.00585.
[18] E. Forestier, C. Combeaud, N. Guigo, G. Monge, J.-M. Haudin, N. Sbirrazzuoli, N. Billon, Strain-induced crystallization of poly(ethylene 2,5-furandicarboxylate). Mechanical and crystallographic analysis, Polymer (Guildf). 187 (2020) 122126, https://doi.org/10.1016/j.polymer.2019.122126.

[19] T.A. Molodtsova, E.V. Boldyreva, V.A. Klushin, Synthesis of poly(ethylene 2,5-Furanoate): I. Kinetics of 2,5-dimethyl Ester of Furandicarboxylic acid transesterification, Mater. Sci. Forum 992 (2020) 311–316, https://doi.org/10.4028/www.scientific.net/MSF.992.311.
[20] S.K. Burgess, R.M. Kriegel, W.J. Koros, Carbon dioxide sorption and transport in amorphous poly(ethylene furanoate), Macromolecules 48 (2015) 2184–2193, https://doi.org/10.1021/acs.macromol.5b00333.
[21] S.K. Burgess, J.E. Leisen, B.E. Kraftschik, C.R. Mubarak, R.M. Kriegel, W.J. Koros, Chain mobility, thermal, and mechanical properties of poly(ethylene furanoate) compared to poly(ethylene terephthalate), Macromolecules 47 (2014) 1383–1391, https://doi.org/10.1021/ma5000199.
[22] G. Guidotti, M. Soccio, M.C. García-Gutiérrez, T. Ezquerra, V. Siracusa, E. Gutiérrez-Fernández, A. Munari, N. Lotti, Fully biobased Superpolymers of 2,5-Furandicarboxylic acid with different functional properties: from rigid to flexible, high performant packaging materials, ACS Sustain. Chem. Eng. 8 (2020) 9558–9568, https://doi.org/10.1021/acssuschemeng.0c02840.
[23] S. Thiyagarajan, A. Pukin, J. van Haveren, M. Lutz, D.S. van Es, Concurrent formation of furan-2,5- and furan-2,4-dicarboxylic acid: unexpected aspects of the Henkel reaction, RSC Adv. 3 (2013) 15678–15686, https://doi.org/10.1039/C3RA42457J.
[24] T.P. Kainulainen, T.A.O. Parviainen, J.A. Sirviö, L.J.R. McGeachie, J.P. Heiskanen, High oxygen barrier polyester from 3,3′-Bifuran-5,5′-dicarboxylic acid, ACS Macro Lett. 12 (2023) 147–151, https://doi.org/10.1021/acsmacrolett.2c00743.
[25] A.M. Ahmed, T.P. Kainulainen, J.A. Sirviö, J.P. Heiskanen, Renewable furfural-based polyesters bearing sulfur-bridged Difuran moieties with high oxygen barrier properties, Biomacromolecules 23 (2022) 1803–1811, https://doi.org/10.1021/acs.biomac.2c00097.
[26] M.M. Nolasco, L.C. Rodrigues, C.F. Araújo, M.M. Coimbra, P. Ribeiro-Claro, P. D. Vaz, S. Rudić, A.J.D. Silvestre, C. Bouyahya, M. Majdoub, A.F. Sousa, From PEF to PBF: what difference does the longer alkyl chain make a computational spectroscopy study of poly(butylene 2,5-furandicarboxylate), Front. Chem. 10 (2022), https://doi.org/10.3389/fchem.2022.1056286.
[27] C. Fosse, A. Esposito, S. Thiyagarajan, M. Soccio, N. Lotti, E. Dargent, L. Delbreilh, Cooperativity and fragility in furan-based polyesters with different glycolic subunits as compared to their terephthalic counterparts, J. Non-Cryst. Solids 597 (2022) 121907, https://doi.org/10.1016/j.jnoncrysol.2022.121907.
[28] G. Papamokos, T. Dimitriadis, D.N. Bikiaris, G.Z. Papageorgiou, G. Floudas, Chain conformation, molecular dynamics, and thermal properties of poly(n-methylene 2,5-furanoates) as a function of methylene unit sequence length, Macromolecules 52 (2019) 6533–6546, https://doi.org/10.1021/acs.macromol.9b01320.
[29] L. Genovese, M. Soccio, N. Lotti, A. Munari, A. Szymczyk, S. Paszkiewicz, A. Linares, A. Nogales, T.A. Ezquerra, Effect of chemical structure on the subglass relaxation dynamics of biobased polyesters as revealed by dielectric spectroscopy: 2,5-furandicarboxylic acid vs. trans-1,4-cyclohexanedicarboxylic acid, Phys. Chem. Chem. Phys. 20 (2018) 15696–15706, https://doi.org/10.1039/C8CP01810C.
[30] M. Soccio, D.E. Martínez-Tong, G. Guidotti, B. Robles-Hernández, A. Munari, N. Lotti, A. Alegria, Broadband dielectric spectroscopy study of biobased poly (alkylene 2,5-furanoate)s' molecular dynamics, Polymers (Basel). 12 (2020) 1355, https://doi.org/10.3390/polym12061355.
[31] O. Gálvez, O. Toledano, F.J. Hermoso, A. Linares, M. Sanz, E. Rebollar, A. Nogales, M.C. García-Gutiérrez, G. Santoro, I. Irska, S. Paszkiewicz, A. Szymczyk, T. A. Ezquerra, Inter and intra molecular dynamics in poly(trimethylene 2,5-furanoate) as revealed by infrared and broadband dielectric spectroscopies, Polymer (Guildf). 268 (2023) 125699, https://doi.org/10.1016/j.polymer.2023.125699.
[32] A. Bourdet, S. Araujo, S. Thiyagarajan, L. Delbreilh, A. Esposito, E. Dargent, Molecular mobility in amorphous biobased copolyesters obtained with 2,5- and 2,4-furandicarboxylate acid, Polymer (Guildf). 213 (2021) 123225, https://doi.org/10.1016/j.polymer.2020.123225.
[33] A. Bourdet, A. Esposito, S. Thiyagarajan, L. Delbreilh, F. Affouard, R.J.I. Knoop, E. Dargent, Molecular mobility in amorphous biobased poly(ethylene 2,5-furandicarboxylate) and poly(ethylene 2,4-furandicarboxylate), Macromolecules 51 (2018) 1937–1945, https://doi.org/10.1021/acs.macromol.8b00108.
[34] M.M. Nolasco, C.F. Araujo, S. Thiyagarajan, S. Rudić, P.D. Vaz, A.J.D. Silvestre, P. J.A. Ribeiro-Claro, A.F. Sousa, Asymmetric Monomer, Amorphous Polymer? Structure–Property Relationships in 2,4-FDCA and 2,4-PEF, Macromolecules 53 (2020) 1380–1387, https://doi.org/10.1021/acs.macromol.9b02449.
[35] S. Zaidi, S. Thiyagarajan, A. Bougarech, F. Sebti, S. Abid, A. Majdi, A.J.D. Silvestre, A.F. Sousa, Highly transparent films of new copolyesters derived from terephthalic and 2,4-furandicarboxylic acids, Polym. Chem. 10 (2019) 5324–5332, https://doi.org/10.1039/C9PY00844F.
[36] S. Thiyagarajan, M.A. Meijlink, A. Bourdet, W. Vogelzang, R.J.I. Knoop, A. Esposito, E. Dargent, D.S. van Es, J. van Haveren, Synthesis and thermal properties of bio-based Copolyesters from the mixtures of 2,5- and 2,4-Furandicarboxylic acid with different diols, ACS Sustain. Chem. Eng. 7 (2019) 18505–18516, https://doi.org/10.1021/acssuschemeng.9b04463.
[37] S. Thiyagarajan, W. Vogelzang, R.J.I. Knoop, A.E. Frissen, J. van Haveren, D.S. van Es, Biobased furandicarboxylic acids (FDCAs): effects of isomeric substitution on polyester synthesis and properties, Green Chem. 16 (2014) 1957–1966, https://doi.org/10.1039/C3GC42184H.
[38] T. Pan, J. Deng, Q. Xu, Y. Zuo, Q.-X. Guo, Y. Fu, Catalytic conversion of furfural into a 2,5-Furandicarboxylic acid-based polyester with Total carbon utilization, ChemSusChem 6 (2013) 47–50, https://doi.org/10.1002/cssc.201200652.
[39] E. Bianchi, M. Soccio, V. Siracusa, M. Gazzano, S. Thiyagarajan, N. Lotti, Poly (butylene 2,4-furanoate), an added member to the class of smart furan-based polyesters for sustainable packaging: structural isomerism as a key to tune the final properties, ACS Sustain. Chem. Eng. 9 (2021) 11937–11949, https://doi.org/10.1021/acssuschemeng.1c04104.
[40] G. Guidotti, M. Soccio, M.C. García-Gutiérrez, E. Gutiérrez-Fernández, T. A. Ezquerra, V. Siracusa, A. Munari, N. Lotti, Evidence of a 2D-ordered structure in biobased poly(pentamethylene furanoate) responsible for its outstanding barrier and mechanical properties, ACS Sustain. Chem. Eng. 7 (2019) 17863–17871, https://doi.org/10.1021/acssuschemeng.9b04407.
[41] R. Androsch, M. Soccio, N. Lotti, D. Cavallo, C. Schick, Cold-crystallization of poly (butylene 2,6-naphthalate) following Ostwald's rule of stages, Thermochim. Acta 670 (2018) 71–75, https://doi.org/10.1016/j.tca.2018.10.015.
[42] Q. Ding, M. Soccio, N. Lotti, N. Mahmood, D. Cavallo, R. Androsch, Crystallization of poly(butylene 2,6-naphthalate) containing diethylene 2,6-naphthalate constitutional defects, Polym. Cryst. 2 (2019) 1–10, https://doi.org/10.1002/pcr2.10044.
[43] S. Quattrosoldi, R. Androsch, A. Janke, M. Soccio, N. Lotti, Enthalpy relaxation, crystal nucleation and crystal growth of biobased poly(butylene isophthalate), Polymers (Basel). 12 (2020), https://doi.org/10.3390/polym12010235.
[44] R. Androsch, M. Soccio, N. Lotti, D. Jehnichen, M. Göbel, C. Schick, Enthalpy of formation and disordering temperature of transient monotropic liquid crystals of poly(butylene 2,6-naphthalate), Polymer (Guildf). 158 (2018) 77–82, https://doi.org/10.1016/j.polymer.2018.10.037.
[45] Q. Ding, D. Jehnichen, M. Göbel, M. Soccio, N. Lotti, D. Cavallo, R. Androsch, Smectic liquid crystal Schlieren texture in rapidly cooled poly(butylene naphthalate), Eur. Polym. J. 101 (2018) 90–95, https://doi.org/10.1016/j.eurpolymj.2018.02.010.
[46] S. Quattrosoldi, N. Lotti, M. Soccio, C. Schick, R. Androsch, Stability of crystal nuclei of poly (butylene isophthalate) formed near the glass transition temperature, Polymers (Basel). 12 (2020) 1099, https://doi.org/10.3390/polym12051099.
[47] Q. Ding, M. Soccio, N. Lotti, D. Cavallo, R. Androsch, Melt crystallization of poly (butylene 2,6-naphthalate), Chinese, J. Polym. Sci. 38 (2020) 311–322, https://doi.org/10.1007/s10118-020-2354-5.
[48] A. Künkel, J. Becker, L. Börger, J. Hamprecht, S. Koltzenburg, R. Loos, M.B. Schick, K. Schlegel, C. Sinkel, G. Skupin, M. Yamamoto, Polymers, biodegradable, in: Ullmann's Encycl. Ind. Chem, Wiley-VCH Verlag GmbH & Co. KGaA, Weinheim, Germany, 2016, pp. 1–29, https://doi.org/10.1002/14356007.n21_n01.pub2.
[49] Y.S. Hu, V. Prattipati, S. Mehta, D.A. Schiraldi, A. Hiltner, E. Baer, Improving gas barrier of PET by blending with aromatic polyamides, Polymer (Guildf). 46 (2005) 2685–2698, https://doi.org/10.1016/j.polymer.2005.01.056.
[50] G.L. Robertson, Food Packaging - Principles and Practice, CRC Press, 2013.
[51] L.W. McKeen, Polyester Plastics, in: Permeability Prop. Plast. Elastomers, Elsevier, 2017, pp. 95–114, https://doi.org/10.1016/B978-0-323-50859-9.00006-3.